Developmental changes in bone mechanics from Florida manatees (*Trichechus manatus latirostris*), obligate swimming mammals

Ingle DN and Porter ME

Department of Biological Sciences, Florida Atlantic University, Boca Raton, FL 33431

Summary Statement: Bone mechanical behavior varies among vertebral column regions, between sexes, and over development in manatees, which are undulatory swimmers that live in neutrally or near-neutrally buoyant conditions.

ABSTRACT

Mammals living in aquatic environments load their axial skeletons differently than their terrestrial counterparts. The structure and mechanical behavior of trabecular bone can be especially indicative of varying habitual forces. Here, we investigate vertebral trabecular bone mechanical properties (yield strength, stiffness, and toughness) throughout development in Florida manatees (*Trichechus manatus latirostris*), obligate undulatory swimmers. Thoracic, lumbar, and caudal vertebrae were dissected from manatees (N=20) during necropsies. We extracted 6 mm^3 samples from vertebral bodies and tested them in compression in three orientations (rostrocaudal, dorsoventral, and mediolateral) at 2 mm min^{-1}. We determined variation in mechanical properties between sexes, and among developmental stages, vertebral regions, and testing orientations. We also investigated the relationships between vertebral process lengths and properties of dorsoventrally and mediolaterally-tested bone. Rostrocaudally-tested bone was the strongest, stiffest, and toughest, suggesting that this is the principle direction of stress. Our results showed that bone from female subadults was stronger and stiffer than their male counterparts; based on these data we hypothesize hormonal shifts at sexual maturity may partially drive these differences. In calves, bone from the posterior region was stronger and tougher than from the anterior region. We hypothesize that since animals grows rapidly throughout early development, bone in the posterior region would be the most ossified to support the rostrocaudal force propagation associated with undulatory swimming.

Introduction

The mammalian vertebral column is a structure that experiences differential loading in terrestrial and aquatic environments. Evolutionary transitions between land and water have driven modifications in skeletal mechanical behavior, or bone's response to forces (Boszczyk et al., 2001; Currey, 1984; Putz and Muller-Gerbl, 1996). The relationships between bone form and function are well documented in terrestrial quadrupeds, whose vertebral columns stretch between weight-bearing pectoral and pelvic girdles that are the primary support against gravity, much like a suspension bridge extending between pillars (Boszczyk et al., 2001; Kardong, 2009; Wainwright et al., 1976). Terrestrial mammalian bone has been shown to form trabeculae (osseous struts) that orient along the principle direction of stress produced during locomotion. However, information is lacking in mammalian species that are secondarily adapted to aquatic environments; swimmers must be able to resist hydrostatic, drag, and lift forces in a denser fluid medium, but through the support of water's buoyant forces, are relieved from a weight-bearing existence (Fish, 2016; Thewissen and Fish, 1997).

Skeletal changes are most extreme in fully aquatic mammals, who cannot support their body weight on land and instead rely on dorsoventral displacement of their axial body to propel themselves through the water column (Berta et al., 2005; Domning and de Buffrenil, 1991; Fish, 1996; Fish, 2016; Thewissen and Fish, 1997). For example, manatees (Order Sirenia) are fully aquatic mammals that swim using whole-body undulations, or bending of the axial body in a posteriorly-traveling wave. The dorsal position of the lungs and pachyosteosclerotic rib bones help maintain neutral buoyancy (Hartman, 1979; Kojeszewski and Fish, 2007). Anatomical investigations have led to functional hypotheses about body movement during undulatory swimming. Such movement patterns may be facilitated by anatomical specializations that produce trade-offs in body flexibility and rigidity between axial regions. These skeletal features act in concert to either enhance or reduce displacement between adjacent vertebrae (Buchholtz, 2001, 2007; Buchholtz and Shur, 2004; Long et al. 1997; Pabst, 2000; Slijper, 1936; Smith et al. 1976; Webb and de Buffrenil, 1990). However, the extent that bone material properties and morphology contribute to the functional performance of manatees has not yet been tested.

Over the course of a lifetime, bone at the material level is dynamic and changes with repetitive loading (Currey, 1984; Lieberman, 1997; Ruff and Runestad, 1992). Force-induced modifications in bony architecture are described by Wolff's Law; changes in stress on the bone cause structural changes, hence organization reflects function (Wolff, 1870). Trabecular, or spongy bone, is highly metabolically active and has an annual turnover rate of 25% compared with 2-3% in denser cortical bone, making it an ideal indicator to observe changes in load direction and magnitude (Eriksen, 2010, 1986; Jacobs, 2000). Loading regimes in varying

environments can dramatically change bone mechanical properties (Byron et al., 2011; Ozcivici et al., 2007; Sun et al., 2009; Zernicke et al., 1990). When the femoral mechanical properties of weight-bearing rats were compared to rats exposed to microgravity for a period of two weeks, the weight-bearing femurs were significantly stronger, stiffer, and tougher (Sun et al., 2009). Ontogenetic changes have also been detected in bone properties. For example, human infants are altricial and have limited mobility; human bone properties change most rapidly in the first year of life as mobility develops and the bones are exposed to increasing loads. By contrast, fully aquatic mammals are precocial and fully mobile at birth. Locomotor performance and bone formation among species with varying degrees of precociality and altriciality are important factors to consider for accurate mechanical interpretations (Carrier, 1996; Currey and Pond, 1989; Young et al., 2009). Manatees are precocial at birth, have a relatively long lifespan, and grow at a faster rate than their closely-related long-living terrestrial counterparts, African elephants (*Loxodonta africana*) (Bryden, 1972; Lindeque and van Jaarsveld, 1993; Reynolds III et al., 2009; Schwarz and Runge, 2009; Vergara-Parente et al., 2010). Growth also varies between sexes; females grow more rapidly than males. However, manatee males tend to reach sexual maturity at 2-3 years in contrast to 3-5 years in females (Hernandez et al., 1995; Koelsch, 2001; Marmontel, 1995). As growth continues and skeletal maturity is approached, bone modeling and remodeling processes reach equilibrium; efficient bone architecture has been shown to form closer to adulthood (Gosman and Ketcham, 2009). In concert with trabecular morphology, mechanical properties reflect structural adaptations throughout development (Currey and Pond, 1989; Torzilli et al., 1981).

The aim of the present study was to determine the vertebral trabecular bone mechanics of precocial and obligate swimming Florida manatees. We quantified bone mechanical properties to understand stress at permanent deformation (yield strength, σ_y), resistance to deformation (stiffness, *E)* and the ability to absorb energy (toughness, U_r): among (1) developmental stages, (2) vertebral column regions, (3) testing orientations, and (4) between sexes. We also examined the relationships between bone mechanical properties and vertebral process lengths. Since manatees grow the most through the calf developmental stage, we hypothesized that variation in bone mechanical properties (yield strength, stiffness, and toughness) would be greater between the perinatal and calf manatees. We also expected mechanical properties would increase along the length and be greatest at the posterior end of vertebral column, where axial displacement during swimming is greatest. Since the rostrocaudal direction has been identified as the principle direction of stress in terrestrial mammalian vertebral columns, we expected stronger, stiffer, and tougher bone in this testing orientation (Aiyanger et al., 2014; Borah et al., 2000; Fyhrie and Vashishth, 2000; Mitton et al., 1997; Swartz et al., 1991). Female manatees have a faster growth rate than males, and we hypothesized that female manatee bone would have greater mechanical properties. Finally,

we predicted that longer spinous and transverse processes, which may indicate greater force production, would correlate with greater properties in the dorsoventral and mediolateral axes; respectively. We expected spinous process lengths would change with animal growth because in mammals, vertebral processes do not completely fuse to centra until after the first few years of life (Hautier et al., 2010). We then compared previously documented terrestrial mammalian bone mechanics with results from the present study to consider variations in habitual loads between terrestrial and aquatic habitats.

Materials and Methods

Specimens

We obtained a letter of authorization for Florida manatee (*Trichechus manatus latirostris* [Harlan, 1824]) tissue from the Florida Fish and Wildlife Commission (FWC). Florida manatees are protected under the Marine Mammal Protection Act and are listed as threatened (IUCN, 2019). This work was approved by an Institutional Animal Care and Use tissue protocol from Florida Atlantic University (A(T)17-08).

We grouped five individuals into each of the following development-descriptive categories based on animal length (cm): perinatal (<150 cm: < 1 year), calf (150-236 cm: 1-2 years), subadult (236-265cm: 3-5 years), and adult (<265 cm: 6+ years) (Table S1; Schwarz and Runge, 2009). At least two males and two females were sampled for each developmental stage. Manatee necropsies (N = 20) were performed at the Marine Mammal Pathobiology Lab (MMPL) in St. Petersburg, FL (USA). Florida manatee carcasses ranged from fresh to decomposed. Although some animals were in later stages of decomposition than others, all bones were *in situ* until necropsy at the MMPL. Causes of death for animals in the present study included watercraft collision (N = 3), natural (N = 11), stillborn/perinatal (N = 5), and undetermined (N = 1).

Vertebral sampling

The manatee vertebral column has four regions: cervical (N=6 vertebrae), thoracic (N = 16-18), lumbar (N = 1-3), and caudal (N = 20-24). We excluded the cervical series in this study because it is highly immobile and occasionally fused together (Buchholtz et al., 2007). From each of the 20 animals, we sampled vertebrae from the thoracic (N = 3), lumbar (N = 2) and caudal regions (N = 6; Fig. 1A; Table S1). We selected the thoracic group (T8-T10) from vertebrae directly aligned with the umbilicus and the two cranially-adjacent bones. Manatees have a range of 1-2 lumbar vertebrae and only true lumbar vertebrae (lacking rib articulations and chevron bones) were selected for this study (Buchholtz et al., 2007). We selected caudal vertebrae, Ca2-Ca4, based on the alignment of Ca3 with the anus. The most posteriorly-placed caudal vertebrae Ca6-Ca8 were immediately anterior to the fluke insertion. In this study, we designate the gross anatomical location of the thoracic and lumbar vertebral series

as 'anterior' and the caudal vertebral series as 'posterior.' However, experimentally, the rostrocaudal direction is used to clarify the anatomical orientation during mechanical tests in contrast to the gross anatomical location of the vertebrae *in situ*. Once vertebral segments were dissected from the column, we left axial soft tissue intact to maintain *in vivo* hydration for the underlying bone (An and Draughn, 1999). Vertebral segments were stored in ice during transportation to the testing site (Florida Atlantic University, Boca Raton, FL, USA), where they were refrozen at -20°C. Then, we separated adjacent vertebrae at intervertebral joints and dissected away soft tissue. We wrapped isolated vertebrae in mammalian Ringer's solution-soaked gauze to maintain tissue hydration, stored them in airtight bags, and refroze them at -20°C (Ebbeson et al., 1999). Trabecular bone can be thawed and refrozen again up to five times without a change in the compressive stiffness (Linde and Sorensen, 1993).

Sample preparation

We thawed and measured spinous and transverse processes (mm) of each vertebra (Table S1). Lengths of damaged processes were not included in the study. We then removed spinous processes, transverse processes, and chevron bones from each centrum using a bandsaw. For the thoracic and caudal vertebral series, we cut a 6 mm slice in the frontal plane from the center of each centrum, and then sawed five cubes with 6 mm^3 dimensions from the slice (Fig. 1D; Fig. 1E). If vertebrae were small and there was insufficient bone material to extract 5 cubes from the slice, we extracted as many cubes as possible (Linde and Sorensen, 1993). For this study, all dissected Florida manatees had two lumbar vertebrae. To obtain the three slices required for our experimental design, we prepared samples from L2 using two slices for testing. One calf vertebra (MNW16014; Table S1) from the caudal region was damaged and was excluded from data collection and analysis.

Marrow was not removed from the bone cubes. The mechanical behavior of bone with marrow present only changes at strain rates of 10 mm s^{-1} or higher, and we compressed bone at 2 mm min^{-1} (Carter and Hayes, 1977). To assess bone anisotropy, we used each centrum slice, described above, to test three orientations (Fig. 1E; rostrocaudal, dorsoventral, and mediolateral). We used a sander and dissection scissors to smooth and remove any projecting tissue from the bone cubes; parallel sides remove any potential stress concentrations that may compromise the accuracy of mechanical tests (Cowin, 2001). Bone was irrigated with mammalian Ringer's solution throughout the machining process to maintain tissue hydration prior to mechanical testing.

Mechanical testing

We measured individual trabecular bone cubes with digital calipers (length, width, and height: mm) and stored them in separate cups filled with mammalian Ringer's solution to maintain hydration. We stored them in a 2°C refrigerator for no more than eight hours between sample preparation and mechanical testing. We assigned samples from each vertebra to three

categories (determined by *in vivo* orientation) that indicate which axis was compressed during tests. Bone cubes from the first vertebra of each regional series (three adjacent vertebrae) were tested rostrocaudally. Cubes from the second and third vertebrae from the series was tested dorsoventrally and mediolaterally, respectively (Fig. 1).

We destructively tested samples in compression to yield at a displacement rate of 2 mm min^{-1} using an Instron E1000 material tester (Figure 1E; Figure S1; An and Draughn, 1999). We chose a compressive loading modality since previous studies have shown that bone in compression can withstand higher stresses compared with either tensile or shear forces (White and Panjabi, 1990). We converted force-displacement curves to engineering stress-strain (σ-ε) curves, which standardizes the compressive load (N) by dividing the force by the cross-sectional area (width • height: mm^2) and displacement by dividing the change in length (mm) by the original length (mm). Yield was defined as the point where the sample transitioned from elastic to plastic deformation, as seen on the σ-ε curve (Fig. S1). We calculated stiffness (*E*: Young's Modulus), or the resistance to deformation, as the slope of the steepest point of the linear portion of the σ-ε curve. Yield strength (σ_y) indicates σ when the material transitions from elastic to plastic deformation (stress at permanent deformation). Toughness (U_r) is the ability to absorb energy and was derived as the area under the σ-ε up until a yield behavior (Fig. S1). We calculated mechanical properties using Bluehill Universal Software v.3.67 (Instron, Norwood, MA, USA). Vertebral process morphometrics and mechanical property data are available in the Dryad repository (https://doi.org/10.5061/dryad.j0zpc869n).

Statistical analyses

We used four-way ANOVAs to examine differences in bone yield strength, stiffness, and toughness using developmental stage (perinatal, calf, subadult, and adult; Table S1), region (thoracic, lumbar, and caudal at the anus, and caudal at the fluke insertion; Fig. 1A), sex, and testing orientation (rostrocaudal, dorsoventral, and mediolateral) as main effects. Animal length (cm) was included in the ANOVA models as a covariate to account for variability among individuals. Based on our hypotheses, we examined the following interaction terms: developmental stage*region, developmental stage*sex, and region*orientation. For our models, compressive mechanical properties of bone cubes (n=5 cubes) were averaged to obtain a mean value for each vertebra. For each effects test, we report the F_{stat} and P values, and the Df contributions to the whole model. *Post-hoc* pairwise Tukey tests were conducted to examine differences among significant interaction terms. We performed power analyses, using the means of each vertebra, to ensure we had enough degrees of freedom to account for all our effects and interactions. While statistical tests were run on the mean mechanical

property from each vertebra, our figures show data from each mechanical test to the illustrate the true range of properties in the trabecular component of these bones.

Next, we examined six general linear models (GLMs) to interpret the relationships among yield strength, stiffness, and toughness with vertebral processes length. For each mechanical property, we used a GLM to examine data from bone tested in the dorsoventral orientation paired with spinous process length, and bone tested in the mediolateral orientation paired with transverse process length (average of right and left sides). Each GLM included animal length and vertebral process length as effects, and the vertebral process length*developmental stage interaction was included because we hypothesized there would be different relationships among process lengths and their parallel testing orientations across developmental stages. When the GLM was significant (P<0.05) and vertebral process length was a significant effect, we examined a *post hoc* simple linear regression on bone mechanical properties and vertebral process lengths of all animals in the study. Additionally, to further understand the impacts of developmental stage, if the vertebral process length*developmental stage interaction was significant in the GLM models, we examined four simple linear regressions between bone mechanical properties and vertebral process lengths of animals, one regression for each developmental stage. All simple regressions included animal length as a blocking factor. Statistical tests were performed using JMP v.5.0.1.a (SAS Institute Inc., Cary, NC, USA). While statistical tests used the mean mechanical properties from each vertebra, our figures show data from each mechanical test (n = 5 cubes per vertebra) to the show true range (error bars) of each property.

Results

Yield strength (σ_y) of vertebral bone

Our four-way ANOVA model for yield strength (σ_y) was significant ($F_{28,204}$=16.4632, P<0.0001). Developmental stage (F=6.127, P=0.0005, Df=3), region (F=8.1760, P<0.0001, Df=3), sex (F=6.8604, P=0.0095, Df=1), and testing orientation (F=84.9407, P<0.0001, Df=2) were significant main effects, while the covariate animal length was not significant. Tukey *post hoc* tests of main effects revealed that trabecular bone with the greatest σ_y was from subadults and adults, from the caudal region aligned with the anus, in females, and tested in the rostrocaudal orientation (Fig. 2; Table S2).

For σ_y, the significant interaction terms included: developmental stage*region and developmental stage*sex (F=3.9336, P=0.0001, Df=9 and F=6.1673, P=0.0005, Df=3, respectively). Region*orientation was not a significant interaction term. *Post hoc* Tukey tests showed that calf bone from the posterior region had statistically greater σ_y than bone from the thoracic region (Fig. 2A; Table S3). Female subadult bone σ_y was greater than their male counterparts (Fig. 2B; Table S3).

Our GLM analysis for trabecular bone yield strength (σ_y) tested in the dorsoventral orientation was significant ($F_{5,72}$=6.7128; R^2=0.318; P<0.0001) with a significant effect of animal length (F=5.3587, P=0.0235). Neither the spinous process length main effect nor the spinous process length*developmental stage interaction term was significant; therefore, we did not investigate *post hoc* simple regressions.

Our GLM analysis for mediolaterally-tested bone yield strength (σ_y) was significant ($F_{5,68}$=9.2286; R^2=0.4043; P<0.0001) with a significant effect of transverse process length (F=4.7054, P=0.0336) and transverse process length*developmental stage interaction term (F=3.5004, P=0.02, Df=3). Animal length was not a significant effect. Simple regressions between mediolaterally-tested bone σ_y and transverse process lengths showed a significant positive correlation ($F_{1,72}$=20.5178; P<0.0001; R^2=0.2217; Fig. 5A), and when separated by developmental stage, was significant only in calves ($F_{1,18}$=6.8868; P=0.0184; R^2=0.2717; Fig. 5A).

Stiffness (E) of vertebral bone

Stiffness (E) was significant in the four-way ANOVA model ($F_{28,204}$=11.6529, P<0.0001). Developmental stage (F=3.3145, P=0.0210, Df=3), sex (F=5.0190, P=0.0261, Df=1) and testing orientation (F=82.5318, P<0.0001, Df=2) were significant effects. Region and the covariate animal length was not significant. *Post hoc* Tukey tests of significant main effects showed that the greatest E was in subadults and adults, in females, and tested rostrocaudally (Fig. 3; Table S2).

Developmental stage* region (F=2.9834, P=0.0023, Df=9) was a significant interaction term. We found no significance in developmental stage*sex or orientation*region. *Post hoc* Tukey tests showed that adult trabecular bone E was significantly greater in the caudal region than at the fluke (Fig. 3A; Table S4).

The GLM analysis examining dorsoventrally-tested bone E was significant ($F_{5,72}$=8.3384; R^2=0.3667; P<0.0001). Animal length was significant (F=18.6463, P<0.0001), but the main effect of spinous process length and the spinous process length*developmental stage interaction term were not.

Next, our GLM for bone E tested in the mediolateral orientation was significant ($F_{5,68}$=10.1454; R^2=0.4273; P<0.0001) with a significance for animal length and the transverse process length*developmental stage interaction term (F=5.766, P=0.0191 and F=4.7461, P=0.0046, Df=3). Transverse process length was not a significant effect. When separated by developmental stage, we found a positive correlation between mediolaterally-tested bone E and transverse process length in calves ($F_{1,18}$=12.8894; P=0.0021, R^2=0.4173; Fig. 5B) with no significant correlations in other age groups.

Toughness (U_r) of vertebral bone

Our ANOVA was significant for toughness (U_r) ($F_{28,204}$=6.7266; P<0.0001). Region (F=9.8717, P<0.0001, Df=3) and testing orientation (F=17.4784, P<0.0001, Df=2) were significant main effects. Sex, developmental stage and animal length were not significant. *Post hoc* Tukey tests of main effects showed that bone U_r was greatest from subadults and adults, the caudal region aligned with the anus, and tested in the rostrocaudal orientation (Fig. 4; Table S2).

Significant interaction terms were developmental stage*region (F=2.6721, P=0.0059, Df=9) and developmental stage*sex (F=4.5497, P=0.0041, Df=3). Region*orientation was not significant. *Post hoc* Tukey analyses detailed that calf bone in the posterior region had significantly greater U_r than in the anterior region (Fig. 4A; Table S5). Subadult females and adult males had the greatest bone U_r (Fig. 4B; Table S5).

When assessing dorsoventrally-tested bone U_r, our GLM was not significant ($F_{5,72}$=1.8069; R^2=0.1115; P=0.1223). However, our final GLM on bone U_r tested in the mediolateral orientation was significant ($F_{5,68}$=3.9583; R^2=0.2254; P=0.0033). Animal length, transverse process length, and transverse process length*developmental stage were not significant effects.

Discussion

Loading regimes in varying environments have been shown to dramatically change bone mechanical behavior (Byron et al., 2011; Ozcivici et al., 2007; Sun et al., 2009; Zernicke et al., 1990). The vast majority of our understanding of skeletal loading relates to terrestrial mammals, and is lacking in aquatic axial undulators (Domning and de Buffrenil, 1991; Fish, 1996; Fish, 2016; Thewissen and Fish, 1997; Wainwright, 1976). Here, we investigated compressive mechanical behavior (yield strength, stiffness and toughness) of manatee trabecular bone and found variations among developmental stages, regions of the vertebral column, sex, and testing orientations (Figs. 2-5). We predicted positive relationships between vertebral process lengths and mechanical properties of dorsoventrally and mediolaterally-tested bone, and we found this relationship was significant for yield strength and stiffness in the calf developmental stage (Fig. 7).

Yield strength (σ_y)

In Florida manatees, we found that calf bone yield strength ($σ_y$, stress at permanent deformation) varied regionally; the posterior body had stronger bone than the anterior body (Fig. 1A; Fig. 2A; Table S3). Regional variation may be most pronounced in calves due to muscle and bone mass scaling with rapid increases in body length, which are the most pronounced during the first two years of a manatee's life (Fig. 2A; Schwarz and Runge, 2009; Vergara-Parente et al., 2010). As mechanical demands increase with accelerated growth, axial muscles produce greater propulsive forces, with the highest transmission traveling to the

tail (Domning, 1978; Fish, 2016; Kojeszewski and Fish, 2007). For example, tail muscles (m. *intertransversarius coccygeus, m. sacrococcygeus ventralis medialis,* and *m. sacrococcygeus ventralis lateralis)* have origins and insertions on caudal vertebrae, which must resist permanent material deformation when alternatively loaded in compression and tension through contractions of swimming musculature (Fig. 1A; Domning, 1978; Kojeszewski and Fish, 2007). In the bottlenose dolphin (*Tursiops truncatus*), another species of fully aquatic mammal, the average maximum muscle stress was over 200 times less than the yield strength of vertebral trabecular bone from manatee subadults and adults, we would expect manatee muscle stress to be even lower since dolphins are considered to be faster with a more derived swimming mode (Arthur et al., 2015; Fish, 1996; Fish et al., 2014; Goforth, 1990; Williams et al., 2014). Additional information on the complex tissue interactions among muscle, connective tissue (tendons, ligaments, intervertebral discs), and bone are needed for a comprehensive understanding of axial body stresses generated and translated through swimming.

Since female manatees grow faster than males, we hypothesized female bone would be strongest for each post-perinatal developmental stage (Schwarz and Runge, 2009). Although male calves and subadults were longer than their female counterparts in the present study, female subadults had stronger bone than their male counterparts (Fig. 2; Table S1). We expect hormone levels may partially mediate intersexual discrepancies. As females reach sexual maturity, they may require more calcium to support a developing fetus and for postpartum lactation, which has been shown to influence bone mechanical properties (Glade, 2013; Vajda et al., 2001). For example, the onset of estrogen and other sex steroid secretions in humans stimulates rapid skeletal mineral acquisition that lasts for the subsequent 10 years (Clarke and Khosla, 2010). Since bone strength positively correlates with trabecular number and bone volume fraction, hormone-influenced shifts in the bony architecture may accompany female maturation in preparation to release calcium stores during pregnancy and lactation (Teo et al., 2006). In this study, adult female bone yield strength was smaller than their subadult counterparts, and we know one adult female (MEC5085) was lactating at the time of death (Table S1); however, interpretations are limited since we did not assess architectural parameters or bone calcium content.

Manatee spinous processes are short along the length of the vertebral column and relatively shorter than other mammals, while transverse processes are quite long and robust (Buchholtz et al., 2007). We found that mediolaterally-tested bone yield strength, which is parallel to the longer transverse processes, was significantly greater than the dorsoventral orientation associated with the spinous processes (Fig. 2C; Table S1; Table S2). Transverse process length positively correlated with bone yield strength from mediolateral compression, but when separated by developmental stage, was significant in calves only (Fig. 5A; Table

S1). The longest transverse processes are concentrated near the fluke where muscles insert through tendinous bundles, and greatest bone yield strength increases scale with the rapid skeletal development and body growth in calves (Fig. 1A; Buchholtz et al., 2007; Domning, 1978). Bone compression tested rostrocaudally was the strongest overall, which echoes the findings of previous studies identifying the rostrocaudal orientation as the principle direction of stress in terrestrial mammals (Fig. 2A; Table S2; Aiyanger et al., 2014; Borah et al., 2000; Fyhrie and Vashishth, 2000; Mitton et al., 1997; Swartz et al., 1991).

Stiffness (E)

In adults, the greatest bone stiffness (E, resistance to deformation) was from the anterior body (Fig. 3A; Table S4). Our data suggest that greater trabecular bone stiffness, in concert with pachyosteosclerotic (swollen and dense) ribs and zygapophyses (Fig. 1B; Fig. 1C), may be contributing to the rigidity of the anterior body in mature animals (Buchholtz et al., 2007; de Buffrenil et al., 2010; Hartman, 1979). Furthermore, stiffer vertebral bone is potentially supporting manatee ribs that have healed from physical trauma caused by watercraft collision, the most prevalent human-related cause of death for the Florida manatee (Lightsey et al., 2006). When a rib fractures from blunt force trauma, it forms a bony callus while healing, adding mass to the rib and anterior body of the animal (Clifton, 2005). Although manatee rib bone stiffness (4-18 GPa; Fig. 6) was similar to the limb bones of other mammals, rib strength and toughness values was comparatively lower, suggesting a heightened susceptibility to impact-induced damage (Clifton et al., 2008; Clifton et al., 2008; Yan et al., 2006; Yan et al., 2006). While no vertebrae in the present investigation had signs of remodeled bone due to fracture, bone damage may have been present in the laterally-positioned ribs, which were discarded at necropsy and not examined.

Like yield strength, rostrocaudally-tested bone was the stiffest, indicating that this orientation is the principle direction in which forces translate through the axial body (Fig. 2B; Table S2). We found that calf bone stiffness increased with transverse process length, which may indicate that bone in the posterior body, where the longest transverse processes are concentrated, have the greatest capability to resist deformation during periods of extreme body growth in the manatee (Fig.3B; Fig. 5B; Table S1; Clifton, 2005).

Toughness (U$_r$)

To generate thrust during swimming, the vertebral column flexes and transmits forces to the tail, which imparts that force to the surrounding water (Kojeszewski and Fish, 2007; Lighthill 1960, 1969, 1970). We found that trabecular bone from calf caudal vertebrae was consistently tougher (U$_r$, ability to absorb energy) than thoracic bone, which may be a product of habitual loading throughout growth and development (Fig. 4A; Table S4). Compared with the anterior body, the posterior body has been previously shown to move with a faster velocity during swimming, ultimately producing a greater force (Kojeszewski and Fish, 2007; Lighthill

1960, 1969, 1970). The high ductility and strength that is characteristic of a tough bone may support forces translated to the caudal region in these undulators throughout growth. Although we lack data on muscle stresses generated in undulating manatees, kinematic data reveal that axial displacement increases in amplitude rostrocaudally and is greatest at the tail tip, indicating the direction of force propagation. Bone in the caudal region in a physically immature animal may require the greatest capacity to absorb energy due to this concentration of forces (Kojeszewski and Fish, 2007; Lighthill 1960, 1969, 1970). A comprehensive investigation on muscle stresses and connective tissue mechanical properties of the manatee throughout development would help elucidate the complex interaction between tissues.

Variable vertebral column loading

Water's buoyant forces eliminate the need for animals to use limbs for body structural support (Gray, 1968; Slijper, 1946; Vogel, 2013). To understand the scope of skeletal behavior among terrestrial and aquatic environments, we compared data from the present study with bone stiffness from several species of land mammals (Fig. 6; data from previously published work). In adult manatees, we found that average rostrocaudally-tested vertebral trabecular bone stiffness (354 MPa; Fig. 4) is within the range of mature terrestrial mammals (265-1510 MPa). Aquatic undulators and land mammals experience high axial stresses on their vertebral columns, and stiffer vertebral columns may have similar needs for withstanding material deformation. When manatees load their vertebral columns during undulatory swimming, a stiffer vertebral column would transmit forces more efficiently in the direction of sinusoidal wave propagation, with a relatively lower energy dissipation (McHenry et al., 1995; Pabst, 2000). A stiffer vertebral column may also similarly facilitate locomotion in terrestrial mammals, and provide material support against gravity-imposed bending moments in the dorsoventral plane. During quadrupedal locomotion intervertebral displacement is reduced by structures such as the *funiculus nuchae* in the neck and the *linea alba* in the trunk that provide passive tension to resist the ventral sagging of the vertebral column (Boszczyk et al., 2001; Smit, 2002). In addition, the critical role of limbs in supporting the skeleton is clear; femur stiffnesses reach 32 GPa, over 90 times greater than vertebral bone (Fig. 6). Further mechanical tests on aquatic mammalian vertebrae (ex: Order Cetacea) would provide a better understanding of bone plasticity and range of mechanical behaviors from the axial body of submerged swimmers.

Our results suggest that growth and development are not equal among mammalian precocial young in terrestrial and aquatic environments; young pig bone was almost twice as stiff as in perinatal manatees (180 MPa and 102 MPa, respectively; Fig. 3; Fig. 6). With maturity, pig vertebral trabecular bone stiffness increased by 32%, while manatee adult bone stiffness was 300% greater than their newborn counterparts. When comparing developmental stages within a species, these data show that vertebral bone in precocial terrestrial young is

stiffer to support themselves against gravitational bending moments along the vertebral column. Manatees are long-lived mammals (maximum >60 years), but grow to 83% of their full body length and reach sexual maturity around 36 months (Quintana-Rizzo and Reynolds III, 2008; Reynolds III et al., 2017; Schwarz and Runge, 2009). Since the musculoskeletal system scales with rapid body growth, we hypothesize that the tripling in bone stiffness between young and adult manatees reflects the increased demands to transmit energy more efficiently down the vertebral column during undulation (McHenry et al., 1995; Pabst, 2000). Due to gaps in the literature, developmental variations in altricial mammalian vertebral trabecular bone are unclear; however, femoral (cortical) bone of mature altricial animals was on average almost three times stiffer than their immature conspecifics (Fig. 6). Additional data on developmental changes among altricial species is needed to determine if vertebral trabecular bone mechanical properties scale similarly.

Shifting from gravitational loading conditions to weightlessness can change the mechanical behavior of mammalian skeletons; for example, when micro-gravitational conditions were simulated in rats, bone strength decreased by 40% and stiffness decreased by 50% compared to control animals experiencing terrestrial gravitational loads (Sun et al., 2009). These conditions can be paralleled with the earliest manatee ancestors (such as *Prorastomus sirenoids*), who were amphibious and began experiencing weightlessness as they radiated into their aquatic environments (Sampurna et al., 2014). However, our data show that manatee vertebral bone stiffness is within the range of terrestrial mammals, suggesting that trabecular bony architecture within vertebral columns specifically may not have experienced pressure to change throughout evolutionary time (Fig 3, 6; Aiyanger et al., 2014; Borah et al., 2000; Fyhrie and Vashishth, 2000; Mitton et al., 1997; Swartz et al., 1991). As they became increasingly aquatic, we hypothesize that amphibious manatee ancestor's vertebral bone stiffness and strength would be similar to extant species (Domning and de Buffrenil, 1991; Houssaye et al., 2015). A caveat to consider when drawing these comparisons; the individual life histories of manatees in the present study are largely unknown. We cannot account for variations that have been shown to influence bone function and architecture: hormonal levels, disease and infection, malnutrition, and senescence (Clarke and Khosla, 2010; Farr and Khosla, 2015; Lill et al., 2002; Owen et al., 2015).

Conclusions

This study is the first to investigate fully aquatic mammalian trabecular bone mechanics from the axis of locomotion; the vertebral column. We found significant differences in bone among developmental stages, regions of the vertebral column, sex, testing orientation, and we detected significant interactions among these main effects. Overall, vertebral process length was a poor predictor for mechanical properties of dorsoventrally and mediolaterally-tested bone. We did find positive correlations between transverse process lengths and yield

strength and stiffness in calf vertebral bone. This may be a product of rapid animal growth and greater skeletal loads transmitting to the posterior body, where the longest transverse processes are concentrated. We propose that during the first few years of life, manatee bone is more developed in posterior regions to support rostrocaudal force propagation and increasing bending amplitudes towards the tail tip during swimming. Manatee adults have bone stiffness that falls within the range of previously documented values for terrestrial mammals, suggesting that loading on the vertebral column is similar, although additional data collection is needed. Future investigations on the form and function of aquatic mammalian vertebral trabecular bone can help elucidate mechanical demands on the vertebral column among various degrees of aquatic dependence.

REFERENCES

Aiyanger, A.K., Vivanco, J., Au, A.G., Anderson, P.A., Smith, E.L., and Ploeg, H.L. (2014). Dependence of anisotropy of human lumbar vertebral trabecular bone on quantitative computed tomography-based apparent density. *J Biomech Eng, 136*(9).

An, Y.H. and Draughn, R.A., eds. (1999). *Mechanical Testing of Bone and the Bone-Implant Interface.* CRC press.

Arthur, L. H., Mclellan, W. A., Piscitelli, M. A., Rommel, S. A., Woodward, B. L., Winn, J. P., Potter, C.W. and Ann Pabst, D. (2015). Estimating maximal force output of cetaceans using axial locomotor muscle morphology. *Mar Mamm Sci*, *31*(4), 1401-1426.

Berta, A., Sumich, J. L., and Kovacs, K. M. (2005). Musculoskeletal System and Locomotion. In *Marine mammals: evolutionary biology* (2nd ed., pp. 165-212). Elsevier.

Borah, B., Dufresne, T.E., Cockman, M.D., Gross, G.J., Sod, E.W., Myers, W.R., Combs, K.S., Higgins, R.E., Pierce, S.A., and Stevens, M.L. (2000). Evaluation of changes in trabecular bone architecture and mechanical properties of minipig vertebrae by three-dimensional magnetic resonance microimaging and finite element modeling. *J Bone Miner Res, 15*(9), 1786-1797.

Boszczyk, B.M, Boszczyk, A.A., and Putz, R. (2001). Comparative and functional anatomy of the mammalian lumbar spine. *Anat Rec, 264*,157–168.

Bryden, M.M. 1972. "Growth and Development of Marine Mammals." Pp. 1–79 in *Functional anatomy of marine mammals.* New York: Academic Press.

Buchholtz, E.A. (2007). Modular evolution of the cetacean vertebral column. *Evol Dev, 9*(3), 278–289.

Buchholtz, E.A. (2001). Vertebral osteology and swimming style in living and fossil whales (Order: Cetacea). *J Zool Lond, 253*, 175–190.

Buchhotlz, E.A. and Shur, S.A. (2004). Evolution of vertebral osteology in Delphinidae (Cetacea)." *Zool J Linnean Soc, 140*, 383–401.

Buchholtz, E.A., Booth, A.C. and Webbink, K.E. (2007). Vertebral anatomy in the Florida manatee (*Trichechus manatus latirostris*): a developmental and evolutionary analysis. *Anat Rec, 290*, 624–637.

Byron, C., Kunz, H., Matuszek, H., Lewis, S., & Van Valkinburgh, D. (2011). Rudimentary pedal grasping in mice and implications for terminal branch arboreal quadrupedalism. *J Morph*, *272*(2), 230-240.

Carrier, D.R. (1996). Ontogenetic limits on locomotor performance. *Physiol Zool*, *69*(3), 467-488.

Carter, D.R. and Hayes, W.C. (1977). The compressive behavior of bone as a two-phase porous structure. *J Bone Joint Surg, 59*: 954-962.

Clark, B.L. and Khosla, S. (2010). Female reproductive system and bone. *Arch Biochem Biophys, 503*, 118-128.

Clifton, K.C. (2005). *Skeletal biomechanics of the Florida manatee* (*Trichechus manatus latirsotris*). PhD diss. University of Florida, Gainesville, FL.

Clifton, K.B., Reep, R.L. and Mecholsky, J.J. (2008). Quantitative fractography for estimating whole bone properties of manatee rib bones. *J Mater Sci*, *43*(6), 2026-2034.

Clifton, K. B., Yan, J., Mecholsky Jr, J. J., & Reep, R. L. (2008). Material properties of manatee rib bone. *J Zool, 274*(2), 150-159.

Cowin, SC, ed. 2001. *Bone Mechanics Handbook*. CRC press.

Currey, J.D (2004). Incompatible mechanical properties in compact bone. *J Theor Biol, 231*(4), 569-580.

Currey, J.D. (1984). *The Mechanical Adaptations of Bones*. Princeton: Princeton University Press.

Currey, J.D. (1999). The design of mineralised hard tissues for their mechanical functions. *J Exp Biol*, *202*(23): 3285-3294.

Currey, J.D. and Pond, C.M. (1989). Mechanical properties of very young bone in the axis deer (*Axis axis*) and humans. *J Zool Lond, 218*:59–67.

de Buffrénil, V., Canoville, A., D'Anastasio, R. and Domning, D.P. (2010). Evolution of sirenian
pachyosteosclerosis, a model-case for the study of bone structure in aquatic tetrapods. *J Mamm Evol*, *17*(2), 101-120.

Domning, D.P. (1978). The myology of the Amazonian manatee, *Trichechus inunguis* (Natterer) (Mammalia: Sirenia)." *Acta Amazon, 8*(2),1–100.

Domning, D. P. (1982). Evolution of manatees: a speculative history. *J Paleontol*, 599-619.

Domning, D.P. and de Buffrenil, V. (1991). Hydrostasis in the Sirenia: quantitative data and functional interpretations. *Mar Mammal Sci, 7*(4), 331-368.

Ebbeson, E.N., Thomsen, J.S., Beck-Nielson, H., Nepper-Rasmussen, H.J. and Mosekilde, L. (1999). Lumbar vertebral body compressive strength evaluated by dual-energy x-ray absorptiometry, quantitative computed tomography, and ashing. *Bone, 25*(6), 713–724.

Eriksen E.F. (2010) Cellular mechanisms of bone remodelling. *Rev Endocr Metab Disord, 11*, 219–227.

Eriksen E.F. (1986) Normal and pathological remodeling of human trabecular bone: three dimensional reconstruction of the remodeling sequence in normals and in metabolic bone disease. *Endocr Rev, 7*, 379–408.

Farr, J.N., and Khosla, S. (2015). Skeletal changes through the lifespan—from growth to senescence. *Nat Rev Endocrinol, 11*(9), 513.

Ferguson, V.L., Ayers, R.A., Bateman, T.A., and Simske, S.J. (2003). Bone development and age-related bone loss in male C57BL/6J mice. *Bone, 33*(3), 387-398.

Fish, F.E. (1996). Transitions from drag-based to lift-based propulsion in mammalian aquatic swimming. *Am Zool, 36*,628–641.

Fish, F.E. (2016). Secondary evolution of aquatic propulsion in higher vertebrates: validation and prospect. *Integr Comp Biol, 56*(6): 1285-1297.

Fish, F. E., Legac, P., Williams, T. M., & Wei, T. (2014). Measurement of hydrodynamic force generation by swimming dolphins using bubble DPIV. *J Exp Biol*, *217*(2), 252-260.

Fyhrie, D.P. and Vashishth, D. (2000). Bone stiffness predicts strength similarly for human vertebral cancellous bone in compression and for cortical bone in tension. *Bone, 26*(2), 169-173.

Glade, M.J. (2013). Effects of gestation, lactation, and maternal calcium intake on mechanical strength of equine bone. *J Am Coll of Nutr, 12*(4), 372-377.

Goforth Jr, H. W. (1990). Ergometry (exercise testing) of the bottlenose dolphin. In *The Bottlenose Dolphin* (pp. 559-574). Academic Press.

Gosman, J.H. and Ketcham, R.A. (2009). Patterns in ontogeny of human trabecular bone from SunWatch Village in the prehistoric Ohio Valley: general features of microarchitectural change." *Am J of Phys Anthrop, 138*(3), 318–332.

Gray, J. (1968). *Animal Locomotion*. London: Weidenfeld and Nicholson.

Hartman, D.S. (1979). *Ecology and behavior of the manatee (Trichechus manatees) in Florida*. Sp Pub No. 5 Am Soc of Mammalogists, Ithaca, NY.

Hautier, L., Weisbecker, V., Sanchez-Villagra, M.R., Goswami, A. and Asher, R.J. (2010). Skeletal development in sloths and the evolution of mammal vertebral patterning. *PNAS, 107*(44), 18903-18908.

Hernandez, P., Reynolds III, J.E., Marsh, H., and Marmontel, M. (1995). Age and seasonality in spermatogenesis of Florida manatees. In *Population biology of the Florida manatee*. National Biological Service Information and Technology Report 1. Edited by T.J. O'Shea, B.B. Ackerman, and H.F. Percival. National Biological Service, Washington, D.C. pp. 84–97.

Houssaye, A., Tafforeau, P., De Muizon, C., & Gingerich, P. D. (2015). Transition of Eocene whales from land to sea: evidence from bone microstructure. *PLoS One*, *10*(2), e0118409.

IUCN 2019. The IUCN Red List of Threatened Species. Version 2019-1. http://www.iucnredlist.org. Downloaded on 09 March 2019.

Jacobs, C.R. (2000). The mechanobiology of cancellous bone structural adaptation. *J Rehab Research Devel,* 37, 209-216.

Kardong, K.V. (2009). *Vertebrates: Comparative Anatomy, Function, Evolution*. Boston: McGraw Hill Higher Education.

Koelsch, J. K. (2001). Reproduction in female manatees observed in Sarasota Bay, Florida. *Marine Mammal Science*, *17*(2), 331-342.

Kojeszewski, T. and Fish, F.E. (2007). Swimming kinematics of the Florida manatee (*Trichechus manatus latirostris*): hydrodynamic analysis of a mammalian swimmer." *J Exp Biol, 210*(14), 2411–2418

Lieberman, D.E. (1997). Making behavioral and phylogenetic inferences from homonin fossils: considering the developmental influences of mechanical forces." *Annu Rev of Anthropol, 26*,185–210.

Lighthill, M. J. (1960). Note on the swimming of slender fish. *J Fluid Mech*, *9*(2), 305-317.

Lighthill, M. J. (1969). Hydromechanics of aquatic animal propulsion. *Annu Rev Fluid Mech*, *1*(1), 413-446.

Lighthill, M. J. (1970). Aquatic animal propulsion of high hydrodynamic efficiency. *J Fluid Mech*, *44*, 265-301.

Lightsey, L.D., Rommel, S.A., Costidis, A.M. and Pitchford, T.D. (2006). "Methods used during gross necropsy to determine watercraft-related mortality in the Florida manatee (*Trichechus manatus latirostris*)." *J Zoo Wildl Med, 37*(3), 262-275.

Lill, C. A., Fluegel, A. K., and Schneider, E. (2002). Effect of ovariectomy, malnutrition and glucocorticoid application on bone properties in sheep: a pilot study. *Osteoporos Int, 13*(6), 480-486.

Linde, F. and Sorensen, H.C.F. (1993). The effect of different storage methods on the mechanical properties of trabecular bone." *J Biomech, 26*(10),1249–1252.

Lindeque, M. and van Jaarsveld, S. (1993). Post-natal growth of elephants *Loxodonta africana* in Etosha National Park, Namibia. *J Zool Lond, 229*, 319-330.

Long, H, Pabst, D.A., Shepard, W.R., and Mclellan, W.A. (1997). Locomotor design of dolphin vertebral columns: bending mechanics and bending morphology of *Delphinis delphis*. *J Exp Biol, 200*(1), 65–81.

Marmontel, M. (1995). Age and reproduction in female Florida manatees. In Population biology of the Florida manatee. National Biological Service Information and Technology Report 1. Edited by T.J. O'Shea, B.B. Ackerman, and H.F. Percival. National Biological Service, Washington, D.C. pp. 98–119.

Mitton, D., Rumelhart, C., Hans, D., and Meunier, P.J. (1997). The effects of density and test conditions on measured compression and shear strength of cancellous bone from the lumbar vertebrae of ewes. *Med Eng Phys, 19*(5), 464-474.

Owen, H.C., Vanhees, I., Gunst, J., Van Cromphaut, S., and Van den Berghe, G. (2015). Critical illness-induced bone loss is related to deficient autophagy and histone hypomethylation. *Intensive Care Med Exp*, *3*(1), 19.

Ozcivici, E., Garman, R., and Judex, S. (2007). High-frequency oscillatory motions enhance the simulated mechanical properties of non-weight bearing trabecular bone. *J Biomech*, *40*(15), 3404-3411.

Pabst, D.A. (2000). To bend a dolphin: convergence of force transmission designs in cetaceans and scombrid fishes." *Am Zool, 40*(1), 146–155.

Putz, R.L.V. and Muller-Gerbl, M. (1996). The vertebral column- a phylogenetic failure?" *Clin Anat, 9*(3), 205–212.

Quintana-Rizzo, E., and Reynolds III, J. E. (2008). Regional management plan for the West Indian manatee (*Trichechus manatus*). *Caribbean Environment Programme, United Nations Environment Programme*.

Reynolds III, J.E., Powell, J.A., and Taylor, C.R. (2017). Manatees (Trichechus manatus, T. senegalensis, and T. inunguis). In W.F. Perrin, B. Wursig, and J.G.M. Thewissen (Eds.), *Encyclopedia of marine mammals* (3rd ed., pp. 682-691). Academic Press.

Ruff, C.B. and Runestad, J.A. (1992). Primate limb bone structural adaptations. *Annu Rev Anthropol, 21*, 407–433.

Sampurna, I.P., Saka, I.K., Oka, G.L., Putra, S. (2014). Patterns of growth of Bali cattle body dimensions. *ARPN J Sci Tech, 4*(1), 22-30.

Savage, R.J.G., Domning, D.P. and Thewissen, J.G.M. (1994). Fossil Sirenia of the west Atlantic and caribbean region. V. The most primitive known sirenian, Prorastomus sirenoides Owen, 1855. *J Vert Paleontol, 14*(3), 427-449.

Schwarz, L.K. and Runge, M.C. (2009). Hierarchial Bayesian analysis to incorporate age uncertainty in growth curve analysis and estimates of age from length: Florida manatee (*Trichechus manatus*) carcasses." *Can J Fish Aquat Sci, 66*(10), 1775-1789.

Slijper, E.J. (1936). Die Cetaceen: Vergleichend-Anatomisch Und Systematisch. *Capita Zool, 6–7*,1–590.

Slijper, E.J. (1946). Comparative biological-anatomical investigations on the vertebral column and spinal musculature of mammals. *Tweede sectie, 42*, 1–128.

Smit, T.H. (2002). The use of a quadruped as an *in vivo* model for the study of the spine - biomechanical considerations. *Eur Spine J, 11*, 137-144.

Smith, G.J., Brown, K.W. and Gaskin. D.E. (1976). Functional myology of the harbour porpoise, *Phocoena phocoena*. *Can J Zool, 54*, 716–729.

Su, X.W., Feng, Q.L., Cui, F.Z., and Zhu, X.D. (1997) Microstructure and micromechanical properties of the mid-diaphyses of human fetal femurs. *Connect Tissue Res, 36*(3), 271-286.

Sun, L., Fan, Y., Li, D., Zhao, F., Xie, T., Yang, X., Gu, Z. (2009). Evaluation of the mechanical properties of rat bone under simulated microgravity using nanoindentation. *Acta Biomater, 5*(9), 3506-3511.

Teo, J.C.M., Si-Hoe, K.M., Keh, J.E.L. and Teoh, S.H. (2006). Relationship between CT intensity, microarchitecture, and mechanical properties of porcine vertebral cancellous bone. *Clin Biomech, 21*, 235-244.

Thewissen, J.G.M. and Fish, F.E. (1997). Locomotor evolution in the earliest cetaceans: functional model, modern analogues, and palaeontological evidence. *Paleobiology, 23*, 482–490.

Torzilli, P.A., Takebe, K., Burstein, A.H. and Heiple, K.G. (1981). Structural properties of immature canine bone. *J Biomech Engin, 103*, 232-238.

Vajda, E.G., Bowman, B.M. and Miller, S.C. (2001). Cancellous and cortical bone mechanical properties and tissue dynamics during pregnancy, lactation, and post-lactation in the rat. *Biol Reprod, 65*(3), 689-695.

Vergara-Parente, J.E., Parenete, C.L. Marmontel, M., Ramos-Silva, J.C. and Bezerra Sa, S. (2010). Growth curve of free-ranging *Trichechus inunguis. Biota Neotrop, 10*(3).

Vogel, S. (2013). *Comparative biomechanics: life's physical world.* Princeton University Press.

Wainwright, S.A., Biggs, W.D., Currey, J.D. and Gosline. J.M. (1976). *Mechanical Designs in Organisms.* New York: John Wiley & Sons.

Webb, P.W. and de Buffrenil, V. (1990). Locomotion in the biology of large aquatic vertebrates. *Trans Am Fish Soc, 119*, 629–641.

White, A. A., and Panjabi, M. M. (1990). *Clinical biomechanics of the spine* (2nd ed.). Philadelphia, PA: JB Lippincott.

Williams, T., W. Friedl and J. Haun. (1993). The physiology of bottlenose dolphins (Tursiops truncatus): Heart rate, metabolic rate and plasma lactate concentration during exercise. *J Exper Biol, 179*, 31–46.

Wolff, J. (1870). Ueber die innere Architectur der Knochen und ihre Bedeutung für die Frage vom Knochenwachsthum. *Archiv für pathologische Anatomie und Physiologie und für klinische Medicin, 50*(3), 389-450.

Yan, J., Clifton, K. B., Mecholsky Jr, J. J., & Reep, R. L. (2006). Fracture toughness of manatee rib and bovine femur using a chevron-notched beam test. *J Biomech, 39*(6), 1066-1074.

Yan, J., Clifton, K.B., Reep, R.L. and Mecholsky, J.J., 2006. Application of fracture mechanics to failure in manatee rib bone. *J Biomech Eng, 128*(3), 281-289.

Yeni, Y. N., & Norman, T. L. (2000). Calculation of porosity and osteonal cement line effects on the effective fracture toughness of cortical bone in longitudinal crack growth. *J Biomed Mater Res, 51*(3), 504-509.

Young, J. W., Fernández, D., & Fleagle, J. G. (2009). Ontogeny of long bone geometry in capuchin monkeys (Cebus albifrons and Cebus apella): implications for locomotor development and life history. *Biol Lett, 6*(2), 197-200.

Zernicke, R. F., Vailas, A. C., Grindeland, R. E., Li, K. C., & Salem, G. J. (1990). Interactive effects of nutrition, environment, and rat-strain on cortical and vertebral bone geometry and biomechanics. *Aviat Space Environ Med, 61*(7), 640-647.

Figures
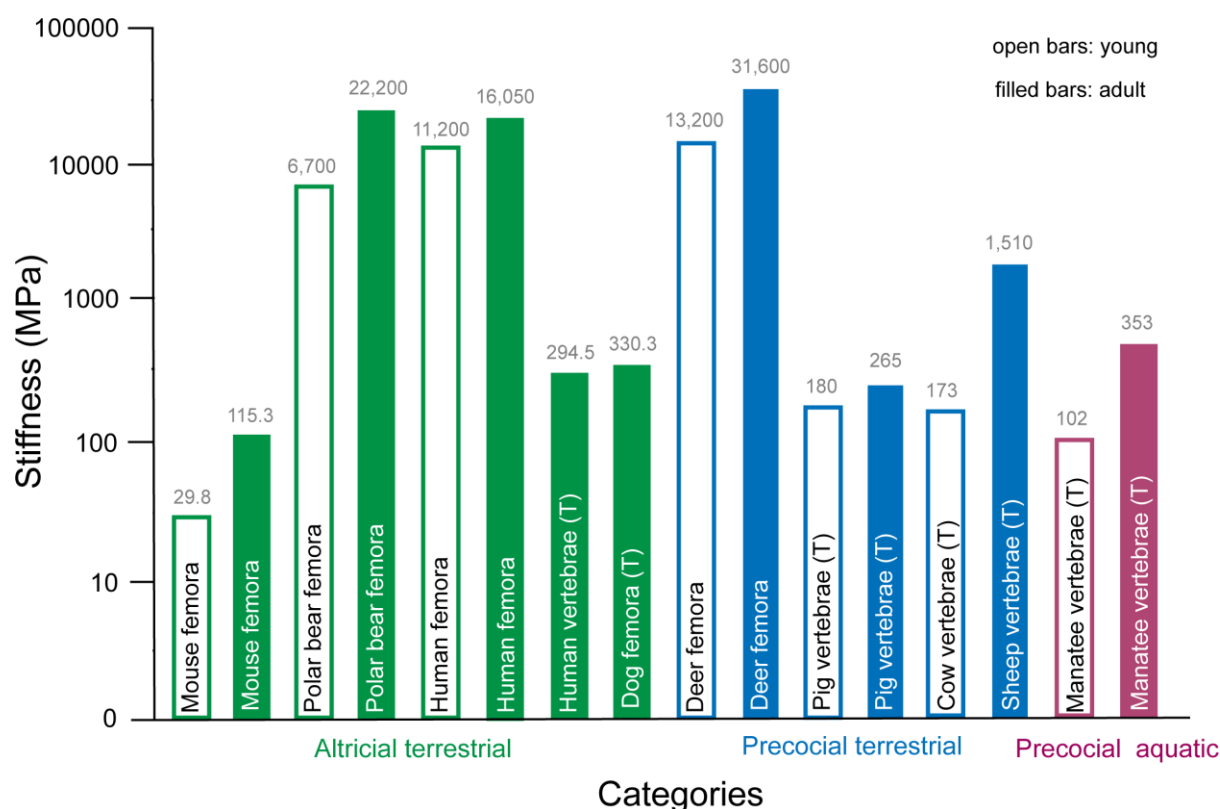
Figure 1. Regional sampling, vertebral anatomy, and sample preparation. (A) Vertebrae were sampled at the (1) thoracic, (2) lumbar, and (3 and 4) caudal regions of the axial vertebrae, which grouped into the anterior (1 and 2) and posterior regions (3 and 4) body. Three adjacent vertebrae were extracted from each region, with the exception of the lumbar region, from which only two vertebrae. (B) Frontal view of a vertebra and its zygaphophyses and transverse processes. (C) Vertebra sagittal view, detailing zygapophyses and the spinous process. Panel photos taken of a subadult Florida manatee thoracic vertebra. Caudal vertebrae in this species lack zygapophyses. (D) Sagittal view. Spinous and transverse processes were removed from the centrum. A 6mm thick slice was machined from the center of each centrum. (E) Frontal view. Five 6mm^3 cubes were cut from the centrum. If size constraints, especially in the perinatal and calf stages, prevented the extraction of five cubes, then as many cubes as possible were machined from each centrum slice.
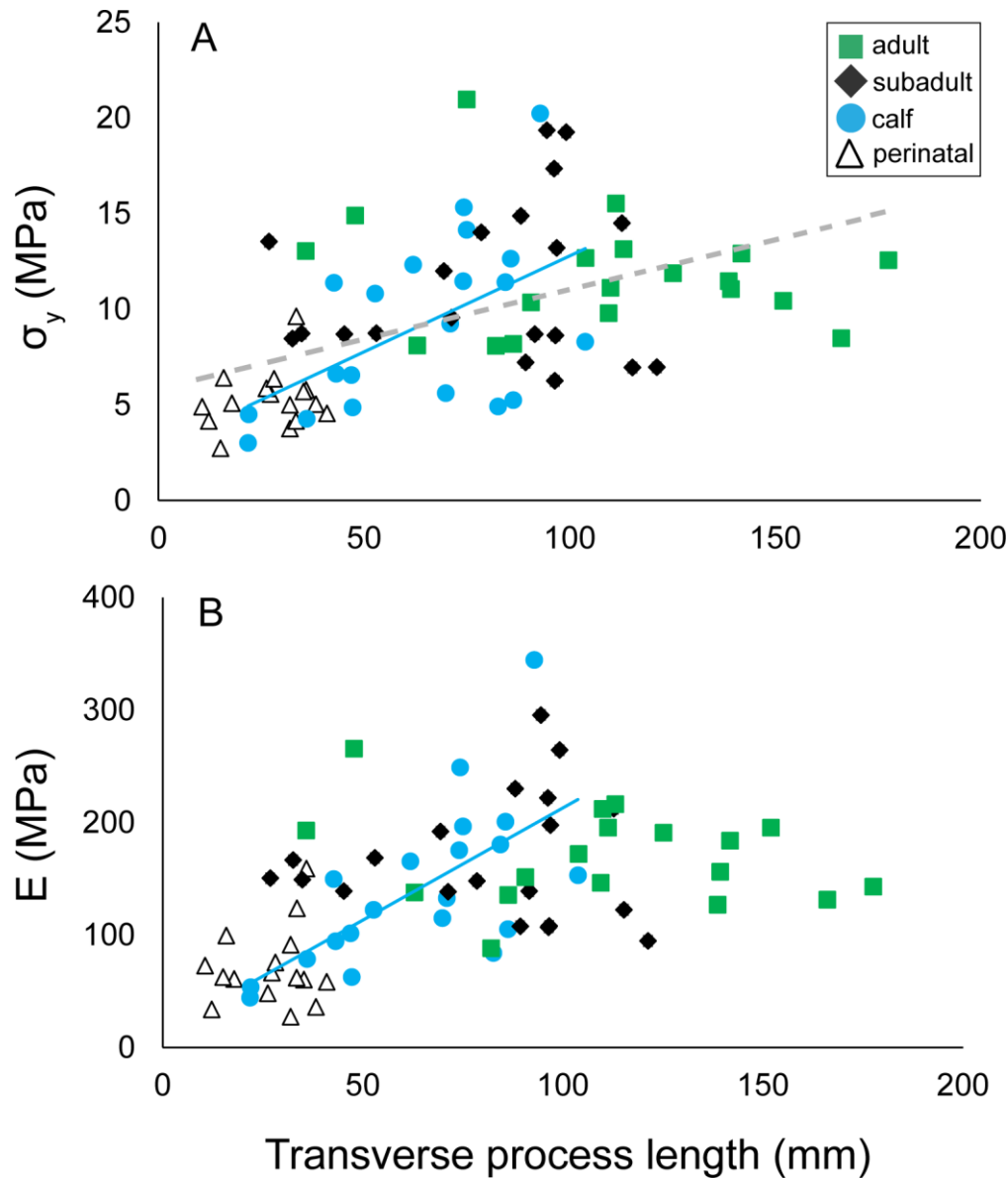
Figure 2. Yield strength (σ_y) of vertebral trabecular bone varied significantly among developmental stages, regions, testing orientations, and between sexes. The following interaction terms were significant in the ANOVA model: developmental stage*region and developmental stage*sex. (A) When examining the developmental stage*region interaction, we found that calf bone σ_y from the posterior region (caudal series) was significantly greater than the thoracic region (P=0.0001). (B) We found that female subadults had greater bone σ_y than their male counterparts (developmental stage*sex: P=0.0005). (C) Rostrocaudally-tested bone had the greatest σ_y (P<0.0001). While statistical tests examined on the mean mechanical property from each vertebra, these figures show data from each mechanical test to the show true range of each property. The center bar in each box denotes the mean, boxes are the 1st and 3rd quartiles, and the whiskers are the minimum and maximum σ_y values. Full Tukey's *post hoc* reports of main effects and interaction terms are in Tables S2 and S3.
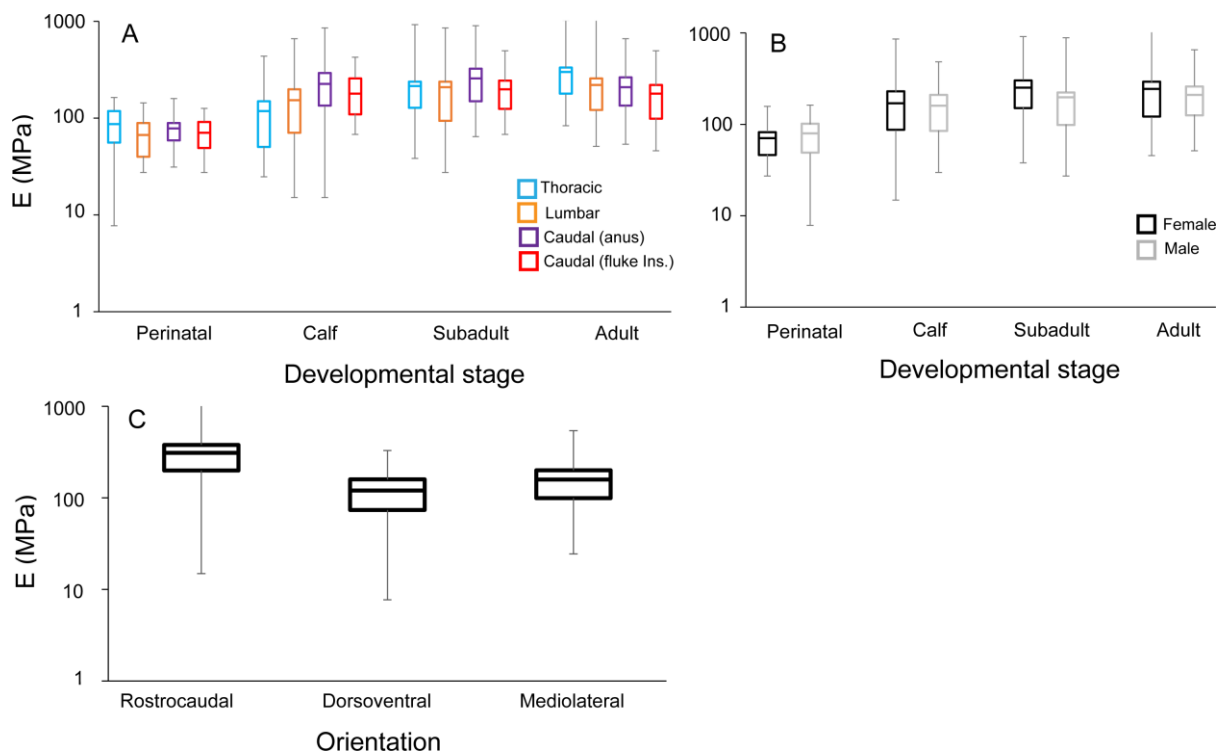
Figure 3. We found variation in trabecular bone stiffness (*E*) of vertebral trabecular bone among developmental stages, testing orientations, and between sexes in the ANOVA model. Developmental stage*region was a significant interaction term. (A) When assessing the developmental stage*region interaction, we found that *E* in adult thoracic bone was significantly greater than caudal bone at the fluke insertion (*P*=0.0023). (B) Females had greater *E* than males (*P*=0.0261). (C) Rostrocaudally-tested bone has the greatest *E* (*P*<0.0001). While statistical tests examined on the mean mechanical property from each vertebra, these figures show data from each mechanical test to the show true range of each property. The center bar in each box denotes the mean, boxes are the 1st and 3rd quartiles, and the whiskers are the minimum and maximum σ_y values. Full Tukey's *post hoc* reports are in Tables S2 and S4.
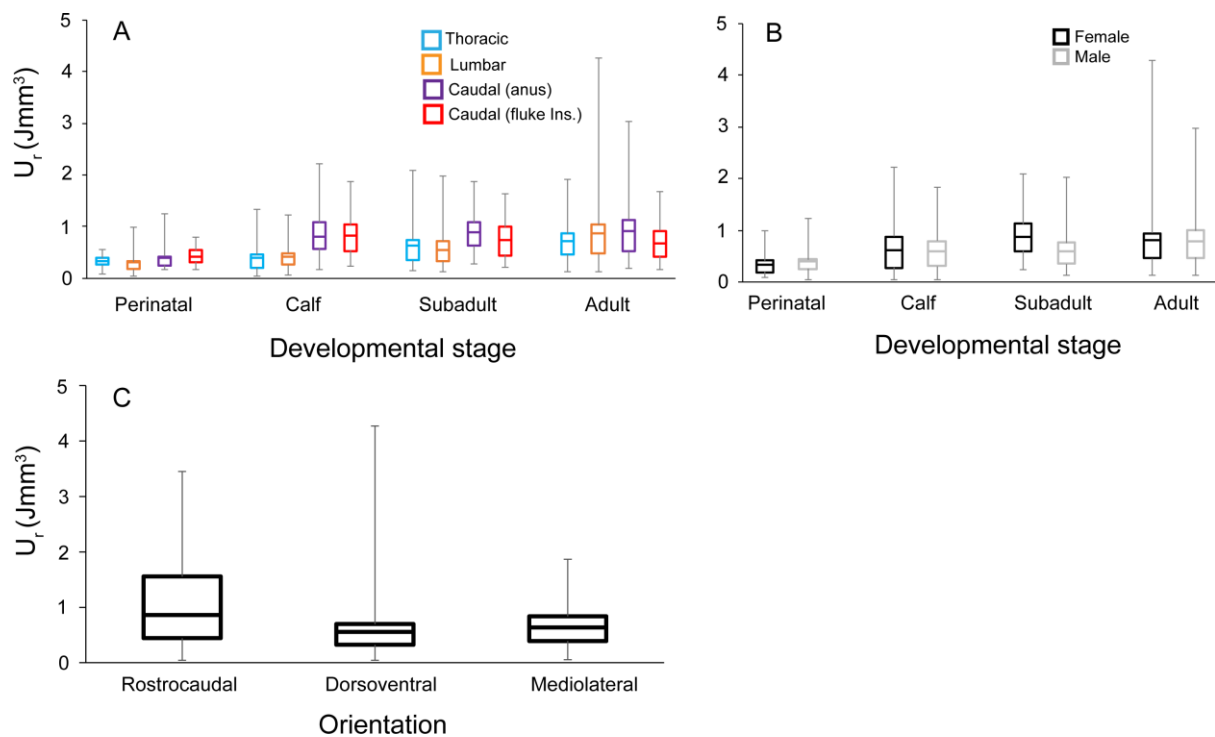
Figure 4. Bone toughness (U_r) varied among regions and testing orientations. The following interaction terms were significant: developmental stage*region and developmental stage*sex. (A) By assessing the developmental stage*region interaction term, we found that calf bone in the posterior region had significantly greater U_r than in the anterior region (P=0.0059). (B) Female subadult bone U_r was significantly greater than their male counterparts (developmental stage*sex: P=0.0041). (C) Bone tested in the rostrocaudal orientation had the greatest U_r (P<0.0001). While statistical tests examined on the mean mechanical property from each vertebra, these figures show data from each mechanical test to the show true range of each property. The center bar in each box denotes the mean, boxes are the 1st and 3rd quartiles, and the whiskers are the minimum and maximum σ_y values. Tukey's *post hoc* reports are in Tables S2 and S5.

A

ANTERIOR   POSTERIOR

1   2   3   4

B
ROSTRAL
Prezygapophyses

Transverse process   Transverse process

Postzygapophyses
CAUDAL

C
DORSAL

Prezygapophyses   Spinous process

Postzygapophyses
VENTRAL

D

6mm

E

6mm

6mm

rostrocaudal
dorsoventral
mediolateral
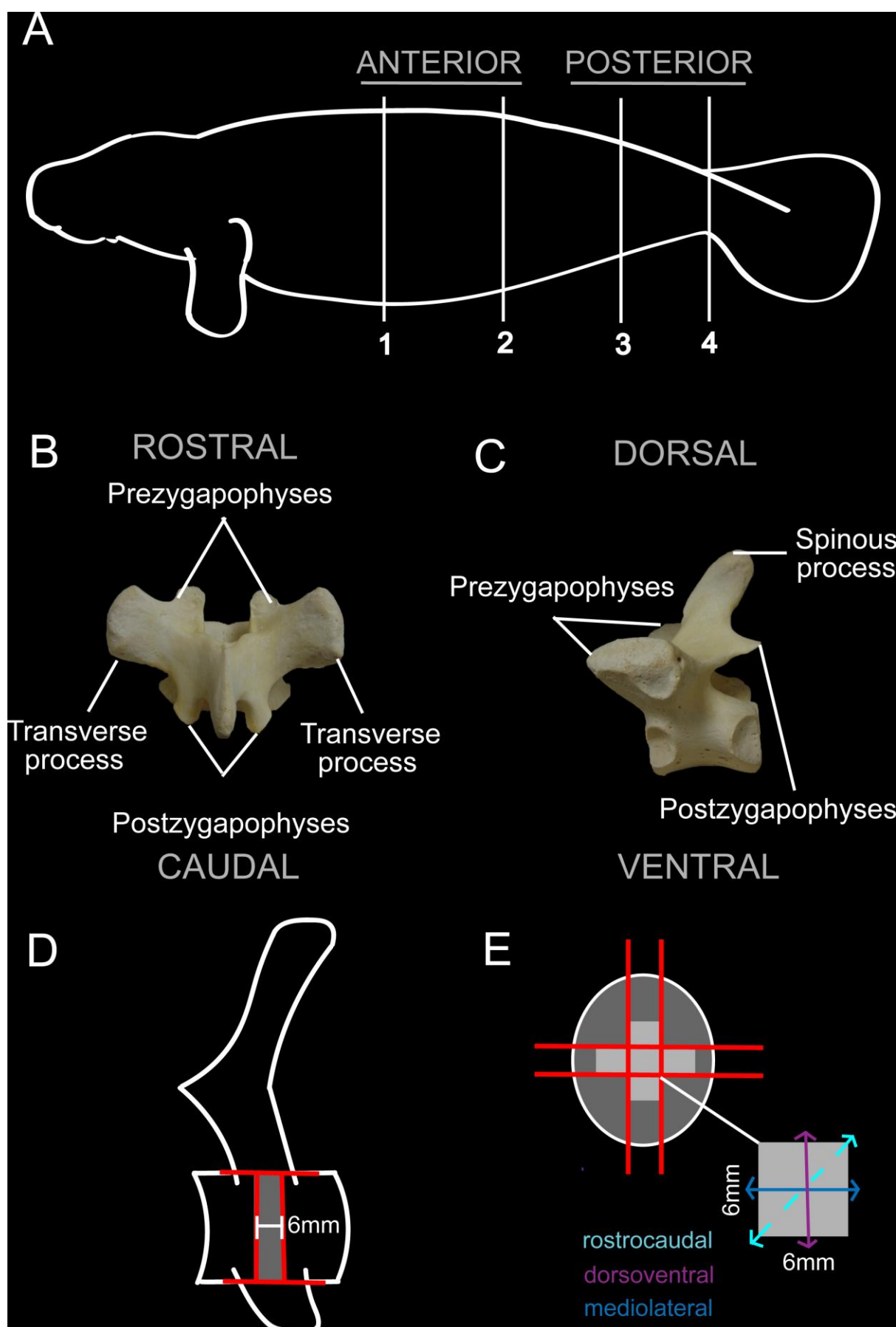
Figure 5. GLMs were used to determine impacts of vertebral process lengths on mechanical properties; simple regressions were only run when the effects of transverse process length or transverse process length*developmental stage were significant. Here, we show linear regressions of bone yield strength and stiffness tested in the mediolateral orientations by transverse process length. (A) For mediolaterally-tested vertebrae from all manatees, bone σ_y increased with transverse process length ($P<0.0001$; $R^2=0.2217$; gray dashed line). When separated by developmental stages, calf bone σ_y increased with transverse process length ($P=0.0184$; $R^2=0.2717$; blue solid line). (B) E positively correlated with transverse process length in calves ($P=0.0021$, $R^2=0.4173$; solid blue line). Each point represents the mean mechanical properties from a single vertebra. For each life stage, we tested four vertebrae from each animal (n = 5).
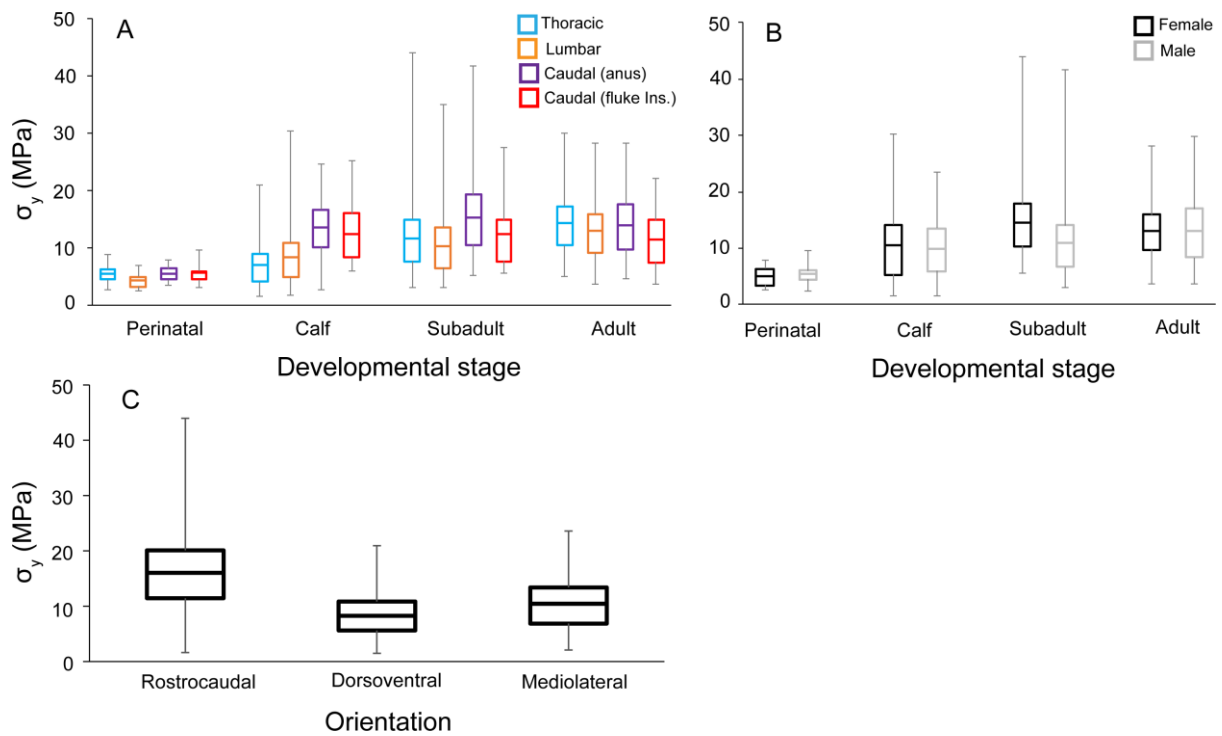
Figure 6. Comparative values of bone stiffness (*E*) among altricial and precocial mammals spanning terrestrial and aquatic environments. Manatee vertebral bone stiffness is from the present study. The young manatee category is represented by perinatal vertebral bone compressed in the rostrocaudal orientation, while the adult group is represented by adult bone tested in the same orientation. In the bar graphs, (T) denotes trabecular bone, and values atop each column are means from the literature and this study (Su et al., 1997; Borah et al., 2000; Swartz et al., 1991; Currey, 1991; Aiyanger et al., 2014; Fyhrie and Vashishth, 2000; Ferguson et al., 2003; Mitton et al., 1997; Turner et al., 1999).

Table S1. Total length, sex, and vertebral process length of 20 manatees sampled for the present study

Developmental stage	Field ID	TL (cm)	Sex	Average vertebral process length (mm)			
				thoracic	lumbar	caudal (anus)	caudal (fluke)
perinatal	MEC16038	113	F	29.85±2.09 17.99±0.48	22.17±1.26 46.61±7.14	23.78±2.27 41.09±0.67	14.94±2.16 36.19±1.37
	MEC16048	130	F	24.09±0.73 18.34±2.53	22.43±0.42 37.88±2.58	16.12±1.49 32.49±2.31	13.76±2.02 33.85±2.49
	MNW16030	118	M	21.33 16.24±0.37	28.52 31.96	13.2±1.31 20.92±5	7.18±0.42 26.27±0.01
	MNW16017	98	M	21.17±0.26 11.72±0.78	28.11±3.98 36.88±4.21	11.35±0.3 28.25±0.72	8.63±1.2 32.18±1.96
	MSW16058	119	M	27.91±0.62 15.86±2.19	23.80±0.44 35.75±2.54	18.11±1.61 36.31±2.68	7.81±1.33 32.44±2.37
calf	MNW16014	209	F	54.99±0.82 34.54±0.66	47.95±3.79 79.8±2.72	44.42±0.25 92.37±1.52	27.56±4.34 61.42±3.8
	MSW16028	192	F	49.26±2.56 24.51±0.92	40.85±5.13 76.4±5.84	34.95±1.84 82.9±4.49	15.16±2.65 53.98±6.74
	MSW16023	185	F	28.60±4.89 22.18±0.66	30.97±4.94 61.53±7.8	14.68±4.29 65.1±1.58	8.37±1.22 47.85±3.13
	MNW16019	206	M	29.58±1.27 46.96±0.74	30.97±4.94 80.99±1.34	14.68 ±4.23 74.76±0.97	8.37±1.22 71.95±0.6
	SWFTM1603b	219	M	60.77±4.79 48.12±1.12	42.59±0.5 84.97±11.29	32.60±2.35 92.09±2.53	16.97±2.03 78.37±1.66
subadult	MEC16019	250	F	62.34±0.49 30.61±1.42	47.43±1.81 84.42±7.28	33.17±1.61 102.18±2.83	18.93±0.13 85.38±2.63
	MEC16022	243	F	40.96±9.51 55.47±0.9	39.98±7.79 88.91±15.18	22.98±4.84 96.99±2.21	14.53±3.88 75.09±3.26
	LPZ103313	256	M	59.41±0.57 31.69±1.01	48.22±0.05 10.3.48±6.71	33.37±0.91 113.88±0.5	19.73±0.41 92.71±0.3
	MNW16018	245	M	59.54±0.84 33.26±0.46	49.95±4.15 96.4±0.47	36.30±2.17 89.16±0.9	17.8±0.48 56.81±8.7
	MNW16021	241	M	67.58±0.15 44.54±0.57	46.60±3.55 99.35±9.21	36.80±2.87 96.93±3.04	16.43±1.64 75.56±1.75
adult	MEC15085	292	F	62.25±0.95 50.26±2.4	46.02±0.71 133.98±2.91	29.74±2.39 117.75±2.69	21.15±4.05 90.65±4.14
	MSW15072	308	F	38.15 43.95	46.98 177.5	28.26±1.54 144.5±1.75	21.75±0.86 117.82±2.64
	MNW16016	310	M	63.08±1.96 68.31±1.25	46.55±1.91 138.2±8.08	37.69±7.11 125.86±6.7	23.69±3.8 122.54±1.8
	MSE16016	308	M	52.65±1.02 69.48±4.13	56.64±4.41 159.75±3.88	36.28±4.39 122.63±8.43	17.31±2.49 89.01±2.88
	MSW16020	287	M	60.90±1.33 34.47±0.28	61.09±1.62 123.46±6.91	36.35±1.28 120.2±2.12	16.27±0.58 96.24±1.37

* TL is total length. Average vertebral process lengths in black text denote spinous process, and in gray text represents transverse process length.

Table S2. Tukey *post hoc* ordered letters report for four-way ANOVA main effects

Main effect		*Post hoc* ordered letters		
		σ_y (MPa)	E (MPa)	U_r (Jmm^3)
developmental stage	perinatal	C	C	C
	calf	B	B	B
	subadult	A	A	A
	adult	A	A	A
region	thoracic	B		C
	lumbar	B		BC
	caudal (anus)	A		A
	caudal (fluke)	AB		AB
orientation	rostrocaudal	A	A	A
	dorsoventral	C	B	B
	mediolateral	B	B	B
sex	female	A	A	
	male	B	B	

*Blanks denote no difference between groups for that mechanical property. Letters that are not A are significantly different from the greatest least squares mean.

Table S3. Tukey *post hoc* ordered letters report for significant interaction terms (developmental stage * region and developmental stage * sex) for σ_y (MPa)

Developmental stage *	Region	*Post hoc* ordered letters
perinatal	thoracic	E
	lumbar	E
	caudal (anus)	E
	caudal (fluke)	E
calf	thoracic	DE
	lumbar	CDE
	caudal (anus)	AB
	caudal (fluke)	ABC
subadult	thoracic	ABC
	lumbar	BC
	caudal (anus)	A
	caudal (fluke)	AB
adult	thoracic	AB
	lumbar	AB
	caudal (anus)	AB
	caudal (fluke)	BCD
Developmental stage *	Sex	
perinatal	female	E
	male	E
calf	female	CD
	male	D
subadult	female	A
	male	BCD
adult	female	ABC
	male	AB

*Letters that are not A are significantly different from the greatest least squares mean.

Table S4. Tukey *post hoc* ordered letters report for significant developmental stage by region interaction term for E (MPa)

Developmental stage *	Region	*Post hoc* ordered letters
perinatal	thoracic	EF
	lumbar	F
	caudal (anus)	EF
	caudal (fluke)	EF
calf	thoracic	DEF
	lumbar	CDEF
	caudal (anus)	ABCD
	caudal (fluke)	BCDE
subadult	thoracic	ABCD
	lumbar	ABCD
	caudal (anus)	AB
	caudal (fluke)	ABCD
adult	thoracic	A
	lumbar	ABC
	caudal (anus)	ABCD
	caudal (fluke)	BCDE

*Letters that are not A are significantly different from the greatest least squares mean.

Table S5. Tukey *post hoc* ordered letters report for significant interaction terms (developmental stage * region and developmental stage * sex) for U_r (Jmm^3)

Developmental stage *	Region	*Post hoc* ordered letters
perinatal	thoracic	F
	lumbar	F
	caudal (anus)	EF
	caudal (fluke)	CDEF
calf	thoracic	F
	lumbar	DEF
	caudal (anus)	ABCD
	caudal (fluke)	ABC
subadult	thoracic	ABCDEF
	lumbar	BCDEF
	caudal (anus)	AB
	caudal (fluke)	ABC
adult	thoracic	ABCDE
	lumbar	AB
	caudal (anus)	A
	caudal (fluke)	ABCDEF
Developmental stage *	Sex	
perinatal	female	D
	male	CD
calf	female	BC
	male	BCD
subadult	female	A
	male	BC
adult	female	AB
	male	A

*Letters that are not A are significantly different from the greatest least squares mean.

Figure S1. Stress-strain curve of an adult Florida manatee's vertebral trabecular bone in compression. Three values were gleaned from each curve: stiffness (E; resistance to deformation), yield strength (σ_y; resistance to permanent deformation) and toughness (U_r; ability to absorb energy up through yield).

Table S1. Total length, sex, and vertebral process length of 20 manatees sampled for the present study

Developmental stage	Field ID	TL (cm)	Sex	Average vertebral process length (mm)			
				thoracic	lumbar	caudal (anus)	caudal (fluke)
perinatal	MEC16038	113	F	29.85±2.09 17.99±0.48	22.17±1.26 46.61±7.14	23.78±2.27 41.09±0.67	14.94±2.16 36.19±1.37
	MEC16048	130	F	24.09±0.73 18.34±2.53	22.43±0.42 37.88±2.58	16.12±1.49 32.49±2.31	13.76±2.02 33.85±2.49
	MNW16030	118	M	21.33 16.24±0.37	28.52 31.96	13.2±1.31 20.92±5	7.18±0.42 26.27±0.01
	MNW16017	98	M	21.17±0.26 11.72±0.78	28.11±3.98 36.88±4.21	11.35±0.3 28.25±0.72	8.63±1.2 32.18±1.96
	MSW16058	119	M	27.91±0.62 15.86±2.19	23.80±0.44 35.75±2.54	18.11±1.61 36.31±2.68	7.81±1.33 32.44±2.37
calf	MNW16014	209	F	54.99±0.82 34.54±0.66	47.95±3.79 79.8±2.72	44.42±0.25 92.37±1.52	27.56±4.34 61.42±3.8
	MSW16028	192	F	49.26±2.56 24.51±0.92	40.85±5.13 76.4±5.84	34.95±1.84 82.9±4.49	15.16±2.65 53.98±6.74
	MSW16023	185	F	28.60±4.89 22.18±0.66	30.97±4.94 61.53±7.8	14.68±4.29 65.1±1.58	8.37±1.22 47.85±3.13
	MNW16019	206	M	29.58±1.27 46.96±0.74	30.97±4.94 80.99±1.34	14.68 ±4.23 74.76±0.97	8.37±1.22 71.95±0.6
	SWFTM1603b	219	M	60.77±4.79 48.12±1.12	42.59±0.5 84.97±11.29	32.60±2.35 92.09±2.53	16.97±2.03 78.37±1.66
subadult	MEC16019	250	F	62.34±0.49 30.61±1.42	47.43±1.81 84.42±7.28	33.17±1.61 102.18±2.83	18.93±0.13 85.38±2.63
	MEC16022	243	F	40.96±9.51 55.47±0.9	39.98±7.79 88.91±15.18	22.98±4.84 96.99±2.21	14.53±3.88 75.09±3.26
	LPZ103313	256	M	59.41±0.57 31.69±1.01	48.22±0.05 10.3.48±6.71	33.37±0.91 113.88±0.5	19.73±0.41 92.71±0.3
	MNW16018	245	M	59.54±0.84 33.26±0.46	49.95±4.15 96.4±0.47	36.30±2.17 89.16±0.9	17.8±0.48 56.81±8.7
	MNW16021	241	M	67.58±0.15 44.54±0.57	46.60±3.55 99.35±9.21	36.80±2.87 96.93±3.04	16.43±1.64 75.56±1.75
adult	MEC15085	292	F	62.25±0.95 50.26±2.4	46.02±0.71 133.98±2.91	29.74±2.39 117.75±2.69	21.15±4.05 90.65±4.14
	MSW15072	308	F	38.15 43.95	46.98 177.5	28.26±1.54 144.5±1.75	21.75±0.86 117.82±2.64
	MNW16016	310	M	63.08±1.96 68.31±1.25	46.55±1.91 138.2±8.08	37.69±7.11 125.86±6.7	23.69±3.8 122.54±1.8
	MSE16016	308	M	52.65±1.02 69.48±4.13	56.64±4.41 159.75±3.88	36.28±4.39 122.63±8.43	17.31±2.49 89.01±2.88
	MSW16020	287	M	60.90±1.33 34.47±0.28	61.09±1.62 123.46±6.91	36.35±1.28 120.2±2.12	16.27±0.58 96.24±1.37

* TL is total length. Average vertebral process lengths in black text denote spinous process, and in gray text represents transverse process length.

Table S2. Tukey *post hoc* ordered letters report for four-way ANOVA main effects

Main effect		*Post hoc* ordered letters		
		σ_y (MPa)	E (MPa)	U_r (Jmm^3)
developmental stage	perinatal	C	C	C
	calf	B	B	B
	subadult	A	A	A
	adult	A	A	A
region	thoracic	B		C
	lumbar	B		BC
	caudal (anus)	A		A
	caudal (fluke)	AB		AB
orientation	rostrocaudal	A	A	A
	dorsoventral	C	B	B
	mediolateral	B	B	B
sex	female	A	A	
	male	B	B	

*Blanks denote no difference between groups for that mechanical property. Letters that are not A are significantly different from the greatest least squares mean.

Table S3. Tukey *post hoc* ordered letters report for significant interaction terms (developmental stage * region and developmental stage * sex) for σ_y (MPa)

Developmental stage *	Region	*Post hoc* ordered letters
perinatal	thoracic	E
	lumbar	E
	caudal (anus)	E
	caudal (fluke)	E
calf	thoracic	DE
	lumbar	CDE
	caudal (anus)	AB
	caudal (fluke)	ABC
subadult	thoracic	ABC
	lumbar	BC
	caudal (anus)	A
	caudal (fluke)	AB
adult	thoracic	AB
	lumbar	AB
	caudal (anus)	AB
	caudal (fluke)	BCD
Developmental stage *	Sex	
perinatal	female	E
	male	E
calf	female	CD
	male	D
subadult	female	A
	male	BCD
adult	female	ABC
	male	AB

*Letters that are not A are significantly different from the greatest least squares mean.

Table S4. Tukey *post hoc* ordered letters report for significant developmental stage by region interaction term for E (MPa)

Developmental stage *	Region	*Post hoc* ordered letters
perinatal	thoracic	EF
	lumbar	F
	caudal (anus)	EF
	caudal (fluke)	EF
calf	thoracic	DEF
	lumbar	CDEF
	caudal (anus)	ABCD
	caudal (fluke)	BCDE
subadult	thoracic	ABCD
	lumbar	ABCD
	caudal (anus)	AB
	caudal (fluke)	ABCD
adult	thoracic	A
	lumbar	ABC
	caudal (anus)	ABCD
	caudal (fluke)	BCDE

*Letters that are not A are significantly different from the greatest least squares mean.

Table S5. Tukey *post hoc* ordered letters report for significant interaction terms (developmental stage * region and developmental stage * sex) for U_r (Jmm^3)

Developmental stage *	Region	*Post hoc* ordered letters
perinatal	thoracic	F
	lumbar	F
	caudal (anus)	EF
	caudal (fluke)	CDEF
calf	thoracic	F
	lumbar	DEF
	caudal (anus)	ABCD
	caudal (fluke)	ABC
subadult	thoracic	ABCDEF
	lumbar	BCDEF
	caudal (anus)	AB
	caudal (fluke)	ABC
adult	thoracic	ABCDE
	lumbar	AB
	caudal (anus)	A
	caudal (fluke)	ABCDEF
Developmental stage *	**Sex**	
perinatal	female	D
	male	CD
calf	female	BC
	male	BCD
subadult	female	A
	male	BC
adult	female	AB
	male	A

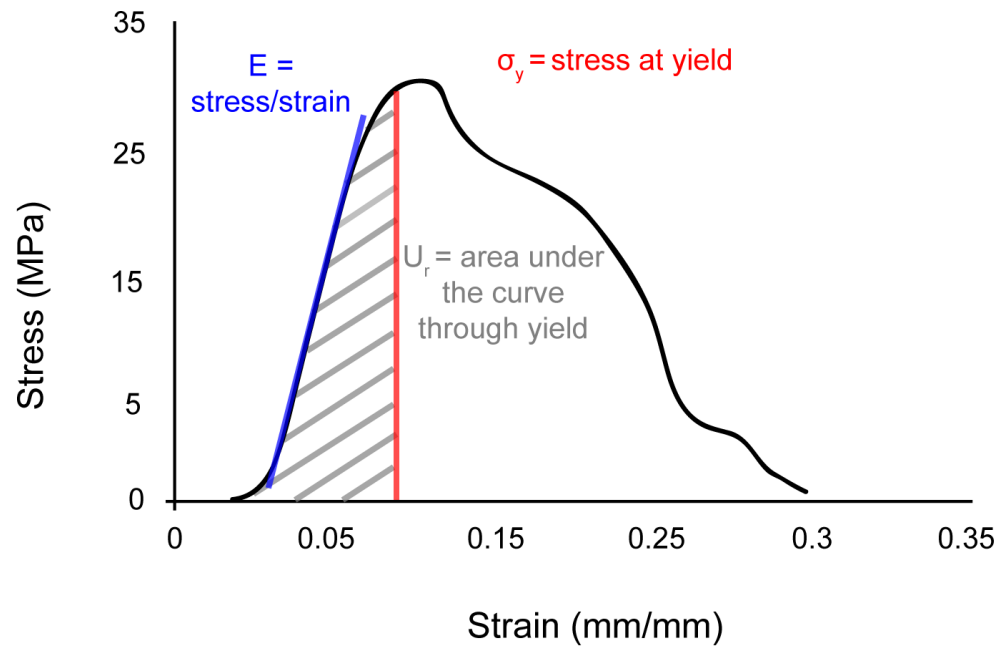*Letters that are not A are significantly different from the greatest least squares mean.

Figure S1. Stress-strain curve of an adult Florida manatee's vertebral trabecular bone in compression. Three values were gleaned from each curve: stiffness (E; resistance to deformation), yield strength (σ_y; resistance to permanent deformation) and toughness (U_r; ability to absorb energy up through yield).